

PAPER • OPEN ACCESS

## Construction of a reduced-order dynamic model for prospective swirling flow control in hydraulic turbine draft tube

To cite this article: Pavel Rudolf *et al* 2019 *IOP Conf. Ser.: Earth Environ. Sci.* **240** 022065

View the [article online](#) for updates and enhancements.

# Construction of a reduced-order dynamic model for prospective swirling flow control in hydraulic turbine draft tube

Pavel Rudolf<sup>1</sup>, Ondřej Urban<sup>1</sup> and David Štefan<sup>1</sup>

<sup>1</sup> V. Kaplan Department of Fluid Engineering, Faculty of Mechanical Engineering, Brno University of Technology, Technická 2896/2, Brno 61669, Czech Republic

Email: rudolf@fme.vutbr.cz

**Abstract.** Vortex rope in Francis turbine draft tubes poses serious problems. Emphasis on operation of the turbines in wide operating range, quite far from the design point, is a challenge for both the turbine designers and power plant owners. While flow control becomes popular in aircraft and automotive industry, it is still feared in turbomachinery. Present paper brings results of investigations aimed on construction of a reduced order model, which describes dynamics of the swirling flow in the draft tube. First step is assessing the dominant modes of the flow, second step is projection of those modes onto a transport equation. Final set of ordinary differential equations is a relatively simple model of the time evolution of the flow dynamics, which is basis for the flow control aiming on mitigation of the instabilities (e.g. vortex rope).

## 1. Introduction

Operation of hydraulic turbines in off-design operating points is associated with highly swirling flows exiting from the runner. This is especially the case for Francis and propeller turbines where the moment of momentum imparted by guide vanes cannot be fully processed by the runner for partload and overload operating points. Resulting swirling flow is susceptible to instabilities of the vortex breakdown type and so-called precessing vortex rope arises for the partload operation (i.e. corkscrew shaped coherent vortical structure rotating with opposite sense than the runner with rotational speed around 1/4th to 1/3rd that of the runner), see figure 1. Vortex rope induces severe pressure pulsations (synchronous and asynchronous), which threaten the turbine operation (increased level of noise and vibrations), operating range limitations and lifetime decrease.

Thorough investigations of this phenomena started in seventies of the 20<sup>th</sup> century employing different analytical tools. Development of advanced experimental and computational methods enabled deeper insight [2, 3] and provided information for more sophisticated analytical approaches [4, 5], but still we are far from complete physical description.

However current situation in energy sector emphasizes the flexibility of hydropower (run-off river, accumulation, pump storage power plants) for control of the electrical grid stability, balancing the load and maintaining the grid frequency. This poses request for turbine operation away from the best efficiency point, i.e. in partload or even no-load conditions.





**Figure 1.** Vortex rope visualization for the part load operation of Francis turbine [1].

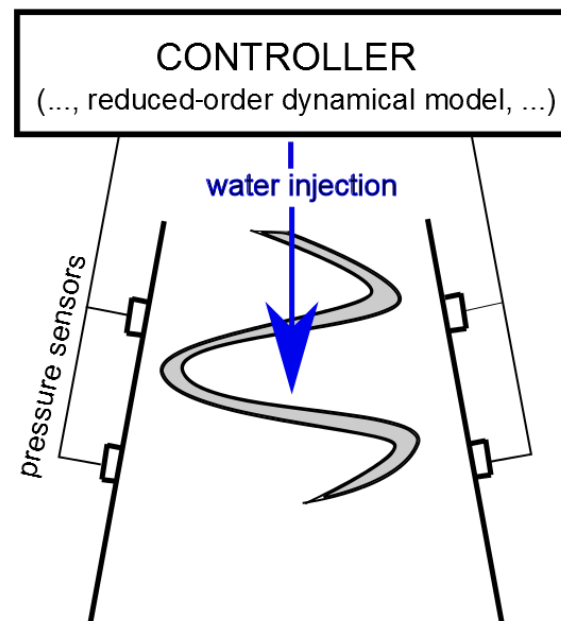


**Figure 2.** Scheme of active closed-loop control of the draft tube flow [9].

## 2. Flow control

Demand on increasing of flow machines parameters and generally parameters of all devices exploiting fluid flow (e.g. increase in efficiency, lower drag, extended operating range, low noise) can be hardly met by mere shape optimization. Therefore different flow control strategies are being developed.

### 2.1. General overview

By flow control is understood manipulation of the flow to suppress undesired flow features: boundary layer separation, vortices, flow recirculations. Historically older and frequently used is passive flow control, i.e. introducing shape modifications or devices, which do not need energy supply (vortex generators on wings, fins limiting inlet recirculation in pumps, car spoilers). Passive control usually has applicability limited to narrow operating range, often at expense of decreasing the device efficiency or other parameters.

Active control devices are usually more complex, but provide the control ability over wider operating range. However energy has to be supplied to such devices from external source (e.g. plasma actuators or synthetic jets on wings). Most of the active control devices are operated in open loop. It means that no feedback information is provided to optimize the energy requirements of the control device according to the actual flow conditions. Recently, closed-loop flow control was suggested for airplanes and cars. Active closed-loop control means real-time adjusting of the flow control according to the feedback from sensors. While this technique is much more complex it can also be much more efficient both in terms of the undesired phenomena suppression over the whole operating range and the energy consumption. Closed-loop control requires not only the actuator for flow manipulation, but also sensors and a control unit. The control unit consists of a controller, whose heart is a reduced order model, which describes the flow dynamics.

## 2.2. Flow control in hydraulic machines

While active flow control becomes increasingly investigated in aerodynamics and gas machines, there are just few examples in hydraulic machines. To illustrate application of active flow control in aircraft industry it is worth mentioning the fluidic nozzle actuators on Boeing airplane tail to suppress flow separations [6] or synthetic jets on highly loaded subsonic compressor cascades [7].

In hydraulic machines air admission through the runner cone for suppression of pressure pulsations is an active control measure. Approach of Resiga [8] with water injection to mitigate vortex rope is also active open-loop control. Active control in hydraulic machines, compared to gas machines, is difficult, because of the working medium density difference. Higher inertia of water poses higher energy requirements on flow manipulation. It should also be admitted that operators' demand on robustness of such control is eligible and presents serious difficulty especially when controlling units with outputs on the order of tens or hundreds of megawatts.

However authors of this believe that closed loop active control is the only way how to further enhance parameters of the hydraulic machines, especially achieving extended operating range. Design of the reduced-order model for the active control of the draft tube flow by water injection is presented. It is the first step to investigate for example intermittent (pulsating) water injection, which might save energy compared to current continuous jet injection, see figure 2.

## 3. Flow decomposition as a prerequisite for reduced-order model construction

To setup the low order dynamical model it is necessary to extract the main flow features, i.e. those flow structures that carry most of the energy. There are several techniques to accomplish this task, proper orthogonal decomposition (POD) being probably the most popular one [10]. A series of so called snapshots (realizations of the flow field in consecutive time instants) has to be supplied for POD [11]. The snapshots can be result of CFD simulation or data from PIV measurements. Advantage of CFD is possibility to provide the data in a 3D domain.

Assume a function  $\mathbf{v} = \mathbf{v}(\mathbf{x}, t)$  (e.g. velocity field), which can be expressed as a sum:

$$\mathbf{v} = \sum_{j=0}^n \boldsymbol{\phi}_j(\mathbf{x}) a_j(t) \quad (1)$$

where  $\boldsymbol{\phi}_j$  is a spatial function (i.e. shape of the POD mode) and  $a_j$  is a temporal function, which describes the temporal evolution of the  $\boldsymbol{\phi}_j$  modes (note: temporal functions  $a_j$  in POD are not pure goniometric functions and can be rather complicated, especially for higher modes). This decomposition is optimal in sense of the least square approximation. Identification of the modes starts with correlation matrix:

$$\mathbf{C}(t, t') = \int_{\Omega} \mathbf{v}(\mathbf{x}, t) \cdot \mathbf{v}(\mathbf{x}, t') d\mathbf{x} \quad (2)$$

The optimization problem (1) leads to Fredholm integral equation:

$$\frac{1}{T} \int_T \mathbf{C}(t, t') a_i(t') dt' = \lambda_i a_i(t) \quad (3)$$

where  $\lambda_i$  is the eigenvalue. Since  $\mathbf{C}$  is positive definite matrix, the eigenvalues  $\lambda_i$  are real positive numbers. If vector  $\mathbf{v}$  corresponds to velocity then components of the correlation matrix  $\mathbf{C}$  correspond to kinetic energy and also  $\lambda_i$  is proportional to kinetic energy of the particular mode. Ranking the eigenvalues according to their magnitude then means ranking of the POD modes according to the kinetic energy they contain. This property enables to identify the most relevant modes for construction of the low-order dynamical model.

More on the POD applied to draft tube vortex rope can be found in [12, 13] and to the mitigation of vortex rope in [14].

#### 4. Reduced-order model

##### 4.1 Reduced-order model by means of traditional Galerkin method

General description of the reduced order model setup can be found in [15]. Assume incompressible Newtonian liquid. The flow of such liquid is governed by the Navier-Stokes equation

$$\frac{\partial \mathbf{v}}{\partial t} + \mathbf{v} \nabla \mathbf{v} = -\frac{1}{\rho} \nabla p + \nu \Delta \mathbf{v} \quad (4)$$

where  $\mathbf{v}$  is the fluid velocity,  $p$  pressure and  $\nu$  kinematic viscosity. The velocity and pressure field can be obtained by CFD modelling or experimental measurements. If we have such data, we can decompose them using numerous techniques to the form

$$\mathbf{v} = \sum_{j=0}^n \boldsymbol{\phi}_j(\mathbf{x}) a_j(t) \quad (5a)$$

$$p = \sum_{j=0}^n \psi_j(\mathbf{x}) a_j(t) \quad (5b)$$

If only  $m$  modes, where  $m \ll n$ , are enough to capture the most important patterns of the flow (coherent structures), it is possible to construct efficient reduced-order model using Galerkin method. First step is to perform Galerkin projection of the Navier-Stokes equation onto the space of  $m$  test functions  $\boldsymbol{\phi}_i$ . To simplify the notation, we set

$$(\mathbf{a}, \mathbf{b})_{\Omega} = \int_{\Omega} \mathbf{a} \cdot \mathbf{b} \, d\Omega \quad (6)$$

Galerkin projection is then defined by

$$\left( \boldsymbol{\phi}_i, \frac{\partial \mathbf{v}}{\partial t} + \mathbf{v} \nabla \mathbf{v} + \frac{1}{\rho} \nabla p - \nu \Delta \mathbf{v} \right)_{\Omega} = 0 \quad (7)$$

In traditional Galerkin projection, (5a) and (5b) are plugged into (4) and  $\boldsymbol{\phi}_i$  is set to be  $\boldsymbol{\phi}_i$ . In general we must consider vectors  $\boldsymbol{\phi}_i$  to be non-orthogonal. Using matrices defined by

$$\hat{m}_{ij} = (\boldsymbol{\phi}_i, \boldsymbol{\phi}_j)_{\Omega}, \quad \hat{l}_{ij} = \frac{1}{\rho} (\boldsymbol{\phi}_i, \nabla \psi_j)_{\Omega} + \nu (\boldsymbol{\phi}_i, \Delta \boldsymbol{\phi}_j)_{\Omega}, \quad \hat{q}_{ijk} = -(\boldsymbol{\phi}_i, \boldsymbol{\phi}_j \nabla \boldsymbol{\phi}_k)_{\Omega} \quad (8)$$

we obtain a set of ordinary differential equations:

$$\sum_{j=0}^m \hat{m}_{ij} \frac{da_j}{dt} = \sum_{j=0}^m \hat{l}_{ij} a_j + \sum_{j,k=0}^m \hat{q}_{ijk} a_j a_k \quad (9)$$

The equation is then multiplied by the inverse of  $\hat{\mathbf{m}}$

$$\frac{da_i}{dt} = \sum_{j=0}^m l_{ij}a_j + \sum_{j,k=0}^m q_{ijk}a_ja_k \quad (10)$$

The zeroth mode  $\phi_0$  is typically the ensemble average. In that case,  $a_0 = 1$  and its time derivative is zero. It is then possible to put the first equation away and in the rest set  $a_0 = 1$ . In this case the model only describes fluctuations of the flow field. After redefinition of matrices

$$c_i = l_{i0} + q_{i00}, \quad l_{ij} = l_{ij} + q_{ij0} + q_{i0j} \quad (11)$$

We obtain the final form

$$\frac{da_i}{dt} = c_i + \sum_{j=1}^m l_{ij}a_j + \sum_{j,k=1}^m q_{ijk}a_ja_k \quad (12)$$

The final modes consist of only  $m$  ordinary differential equation. For flows with dominant coherent structures,  $m$  in order of tens can be enough to obtain reasonable description. The drawback is that the accuracy quickly drops when moving away from the reference point, i.e. the point in which the velocity and pressure data were obtained. Traditional Galerkin models can also suffer from numerical instability as it was shown by Noack et al. 0.

#### 4.2 Application of Galerkin method on vortex rope

The data for POD method were obtained by CFD simulation using the Reynolds-averaged Navier-Stokes equations and the Reynolds stress equation model to model the Reynolds stress tensor components. The spatial domain was the draft tube of swirl generator designed by Resiga et al. [17]. The inlet boundary condition was obtained from CFD simulation of the whole geometry. At the outlet, zero static pressure is prescribed. Flow was simulated as one-phase, without cavitation. A total of 713 snapshots with  $10^{-3}$  s time step were taken for POD analysis. This time interval covers exactly 11 periods of the precessing motion of vortex rope. However, for the simulation itself, the time step was set to  $10^{-4}$  s. In figure 1, the resultant vortex rope is depicted.

In case of RANS simulations of turbulent flow, the transport equation onto which the POD modes should be projected is Reynolds-averaged Navier Stokes equation and not the pure Navier-Stokes equation. Although RSM model was used for the CFD simulation, Boussinesq hypothesis approach is adopted for construction of the reduced model (note: turbulent viscosity can be recovered applying Prandtl-Kolmogorov relation for turbulent kinetic energy (TKE) and turbulent dissipation rate, where TKE is computed from the Reynolds stress tensor components and transport equation for turbulent dissipation rate is part of the RSM model).

$$\frac{\partial \bar{v}}{\partial t} + \bar{v} \nabla \bar{v} = -\frac{1}{\rho} \nabla p + \nu \Delta \bar{v} + \nu_t \Delta \bar{v} + 2\mathbf{S} \nabla \nu_t - \frac{2}{3} \nabla k \quad (13)$$

The last 3 terms in (13) are result of the Boussinesq hypothesis. Overbar stands for averaged values and  $\mathbf{S}$  is the strain rate tensor.

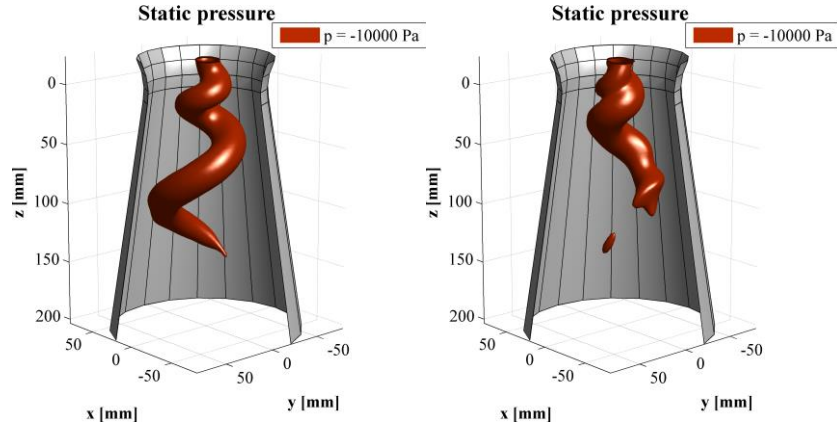


**Figure 3.** Vortex rope visualized by isocontour of static pressure. On the left, the structure is developed and its isocontour is smooth. On the right, the structure itself is undergoing instability.

As the next step, POD of the flow fields was performed. The data matrix was composed as follows

$$A^T = (v_x^T, v_y^T, v_z^T, p^T, v^T, k^T) \quad (14)$$

where T denotes transposition. Turbulent viscosity  $\nu$  and turbulent kinetic energy  $k$  were also included to account for turbulence in the reduced-order model using Boussinesq hypothesis rather than Reynolds stresses. To justify this, it was necessary to check that the difference is negligible. With more than one variable in the data matrix it is suitable to nondimensionalize them. The most important modes of static pressure are depicted in figure 4.

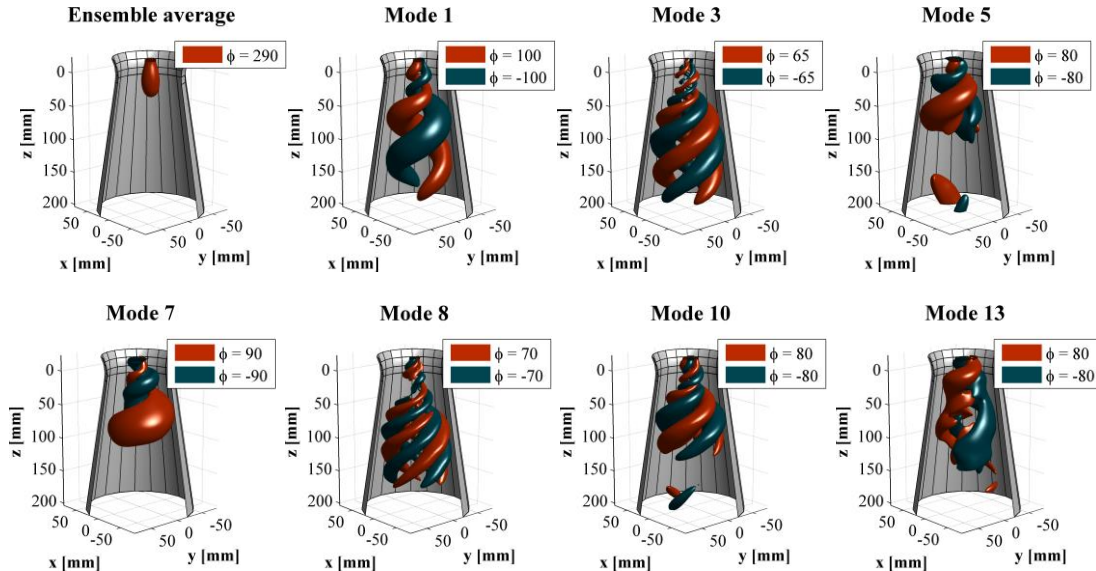


**Figure 4.** Ensemble average and the most important POD modes of static pressure visualized by isocontours. Only one of the pair is depicted.

Importance of modes can be quantified using  $\ell^2$  norm. The dependence of reconstruction accuracy on number of summed most important modes using this norm is depicted in figure 3. It can be seen that

90 % accuracy on average in recovering of the original fields is obtained using 20 modes. The convergence to 100 % from this point is slow. It can be expected that with longer time domain the convergence would be even slower. This is because of the instability of the vortex rope which is not low-dimensional.

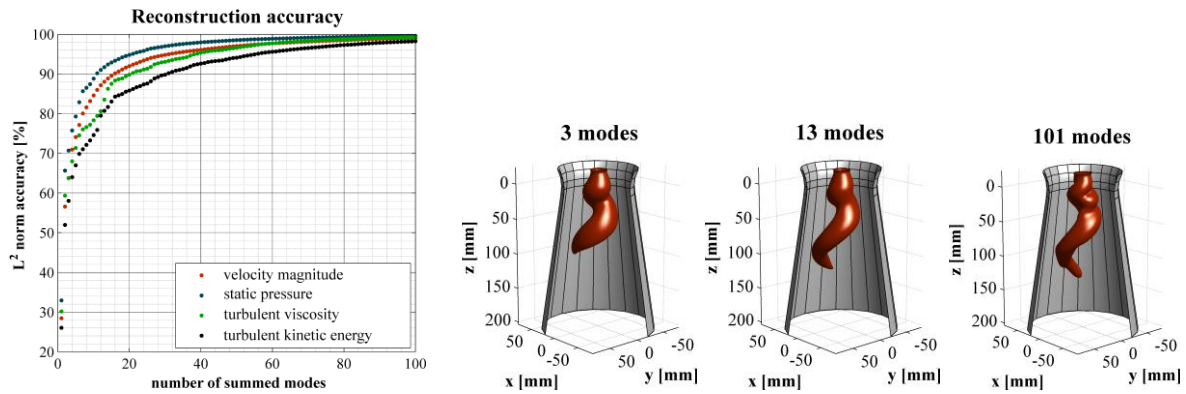


**Figure 5.** Dependence of reconstruction accuracy on number of summed modes (left), reconstruction of vortex rope isocontour (right). Original snapshot is depicted in figure 3.

The reconstruction of static pressure field from figure 5 shows that 13 POD modes are enough to capture the basic structure, but not enough to capture the instabilities. They are reasonably captured with 101 modes summed, but this is only valid for the reference time interval as the dynamics are high-dimensional. It is clear that utilizable reduced-order model will have to ignore not a minor part of the dynamics.

Final step is to perform Galerkin projection of selected number of POD modes onto the Reynolds-averaged Navier-Stokes equation. The model is then solved for the reference point, i.e. the initial condition are the first values of temporal POD modes. Therefore, comparison of them can be used as a measure of accuracy. Results for different number of modes included in the model are depicted in figs. 6 and 7.

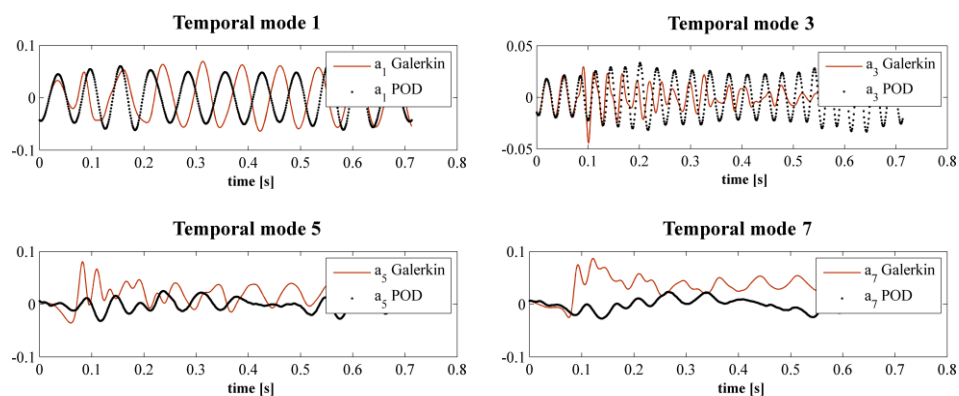


**Figure 6.** Comparison of ROM results with temporal POD modes. Used modes: 15.

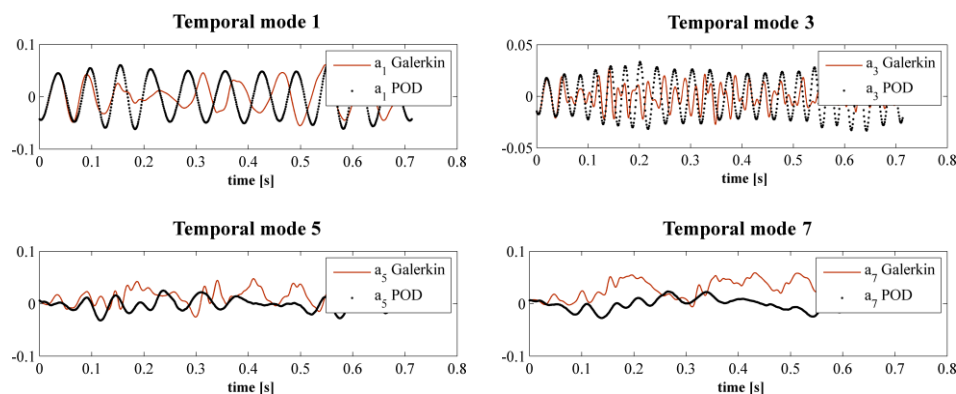


**Figure 7.** Comparison of ROM results with temporal POD modes. Used modes: 30.

It can be seen that the results are reasonably accurate only for rather short time. Then a rapid transition to incorrect attractor occurs. Results of model with 15 modes tend to converge to too simple dynamics whereas model with 30 modes tend to converge to more complicated dynamics. Temporal POD modes (functions  $a_i$ ) are by definition rather complicated and pose a problem in setting up ROM, which correctly evolves in time. This leads to a proposal for using simpler modes (e.g. DMD or Fourier modes), but at the price of higher requirements on the number of modes.

## 5. Conclusion

A procedure for construction of a reduced-order model, which describes the dynamics of the coherent structures within the draft tube for part load turbine operation is described. The resulting ROM is based on POD modes from RANS CFD simulation. Considerable inaccuracy of the model is observed after a short time interval. This discrepancy can be attributed to two facts. First, because RANS simulation was used to set up the POD modes, turbulent viscosity plays significant role. Future work will use POD modes from LES simulation, where most of the flow is directly computed and turbulent viscosity is only on the subgrid level. Second, different forms of decompositions will be tested to overcome troubles with awkward evolution of the temporal mode functions.

It should also be noted that the proposed reduced-order model is only valid in vicinity of the selected operating point. To cover the whole turbine hill chart, it is necessary to include so-called shift modes, which allow to switch between different operating points [15].

## Acknowledgement

This research was supported by Czech Science Foundation under project 17-01088S “3D instability of a shear layer in adverse pressure gradient”.

## References

- [1] Koutník J, Krüger K, Pochylý F, Rudolf P and Habán V 2006 On cavitating vortex rope form stability during Francis turbine part load operation *Proceedings of abstracts Int. Meetings of the Work Group on “ Cavitation and Dynamics Problems in Hydraulic Machinery and Systems”* Barcelona
- [2] Ciocan G D, Iliescu M S, Vu T C, Nenneman B and Avellan F 2007 Experimental study and numerical simulation of the FLINDT draft tube rotating vortex *Journal of Fluids Eng.* **129** pp. 146-158

- [3] Iliescu M S, Ciocan G D and Avellan S 2008 Analysis of the cavitating draft tube vortex in a Francis turbine using particle image velocimetry measurements in two-phase flow *Journal of Fluids Eng.* **130** (2)
- [4] Susan-Resiga R, Muntean S, Avellan F and Anton I 2011 Mathematical modelling of swirling flow in hydraulic turbines for the full operating range *Applied Mathematical Modelling* **35** (10)
- [5] Pochyly F, Cermak L, Rudolf P, Haban V and Koutnik J 2009 Assessment of the Steady Swirling Flow Stability Using Amplitude-Frequency Characteristic, *Proc. of 3rd IAHR International Meeting of the Workgroup on Cavitation and Dynamic Problems in Hydraulic Machinery and Systems* Brno
- [6] Andino M Y, Lin J C, Washburn A E, Whalen E A, Graff E C and Wygnanski I J 2015 Flow Separation Control on a Full-Scale Vertical Tail Model using Sweeping Jet Actuators *Proc. of 53rd AIAA Aerospace Sciences Meeting*
- [7] Zheng X, Zhou S, Lu Y, Hou A and Li Q 2008 Flow control of annular compressor cascade by synthetic jets *Journal of Turbomachinery* **130** (2)
- [8] Tanasa C, Susan-Resiga R, Muntean S and Bosioc A I 2013 Flow-feedback method for mitigating the vortex rope in decelerated swirling flows *Journal of Fluids Engineering* **135** (6)
- [9] Rudolf P, Štefan D and Klas R 2015 Spatio- Temporal Description of the Swirling Flow in Hydraulic Turbine *Wasserwirtschaft* 1 pp 18-22.
- [10] Berkooz H, Holmes P and Lumley J L 1993 The proper orthogonal decomposition in the analysis of turbulent flows *Ann. Rev. Fluid Mechanics* 25
- [11] Sirovich L 1987 *Quarterly of Applied Mathematics* **XLV** 561-71
- [12] Štefan D and Rudolf P 2015 Proper Orthogonal Decomposition of Pressure Fields in a Draft Tube Cone of the Francis (Tokke) Turbine Model *Journal of Physics: Conference Series. Journal of Physics: Conference Series* IOP Publishing pp 1-14
- [13] Rudolf P and Štefan D 2012 Decomposition of the swirling flow field downstream of Francis turbine runner *IOP Conference Series: Earth and Environmental Science* IOP Publishing Ltd. pp 1-8
- [14] Štefan D, Rudolf P, Muntean S and Susan-Resiga R 2017 Proper Orthogonal Decomposition of Self- Induced Instabilities in Decelerated Swirling Flows and Their Mitigation Through Axial Water Injection *Journal of Fluids Engineering* **139** (8) pp 1-25
- [15] Noack B R, Morzyński M and Tadmor G 2011 *Reduced-Order Modelling for Flow Control*, Springer
- [16] Noack B R, Afanasiev K, Morzyński M, Tadmor G and Thiele F 2003 A hierarchy of low-dimensional models for the transient and post-transient cylinder wake *Journal of Fluid Mechanics* **497**
- [17] Susan-Resiga R, Muntean S, Tănasă C and A Bosioc 2008 Hydrodynamic Design and Analysis of a Swirling Flow Generator *Proc. of the 4th German – Romanian Workshop on Turbomachinery Hydrodynamics* Stuttgart